Fracture Toughness of a Hybrid-Rubber-Modified Epoxy. I. Synergistic Toughening

M. Abadyan,[1] R. Bagheri,[2] M. A. Kouchakzadeh[1]

[1]*Engineering Department, Shahrekord Branch, Islamic Azad University, Shahrekord, Iran*
[2]*Department of Materials Science and Engineering, Sharif University of Technology, Azadi Avenue, P.O. Box 11155-9466, Tehran, Iran*

Received 9 December 2008; accepted 29 July 2011
DOI 10.1002/app.35367
Published online 27 Janaury 2012 in Wiley Online Library (wileyonlinelibrary.com).

ABSTRACT: The fracture behavior of a hybrid-rubber-modified epoxy system was investigated. The modified epoxy included amine-terminated butadiene acrylonitrile (ATBN) rubber and recycled tire particles as fine and coarse modifiers, respectively. The results of the fracture toughness (K_{IC}) measurement of the blends revealed synergistic toughening in the hybrid system when 7.5-phr small particles (ATBN) and 2.5-phr large particles (recycled tire) were incorporated. Transmission optical micrographs showed different toughening mechanisms for the blends; fine ATBN particles increased the toughness by increasing the size of the damage zone and respective plastic deformation in the vicinity of the crack tip. However, in the case of hybrid resin, coarse recycled rubber particles acted as large stress concentrators and resulted in the branching of the original crack tip. Mode mixity at the branch tips led to synergistic K_{IC} in the hybrid system. It seemed that the ductility of the matrix played an effective role in the nature of the crack-tip damage zone in the hybrid epoxies. © 2012 Wiley Periodicals, Inc. J Appl Polym Sci 125: 2467–2475, 2012

Key words: fracture; resins; resists

INTRODUCTION

The addition of a second rubbery particulate phase, that is, rubber modification, has been applied to overcome the intrinsic brittleness of epoxy resins.[1–4] Cavitation, void growth, and concomitant plastic deformation of the matrix are believed to be the dominant toughening mechanisms of rubber modifiers for absorbing energy and increasing resin toughness.[5–7] The use of two types of modifiers produces a hybrid system that may promote the simultaneous occurrence of several toughening mechanisms.[8] The fracture toughness (K_{IC}) of the hybrid compound may be higher than that of a single-particle-modified resin. If the toughening mechanisms interact in a positive fashion, a synergistic toughening may be achieved in that, for a given volume fraction of modifiers, K_{IC} of the composition would be greater than additive contributions of the two modifiers separately. There are reports of this synergistic toughening in epoxy systems containing a combination of soft and hard particles, such as rubber and solid glass spheres.[8–10] Kinloch et al.[9] reported synergistic toughening for a hybrid-modified epoxy containing rubber and large solid glass spheres. They observed that K_{IC} of the hybrid modified epoxy was higher than those of either of the formulations containing the individual modifiers. The increase in K_{IC} was claimed to be a result of both the plastic deformation of the matrix and the crack-pinning mechanism being present. Azimi et al.[10] reported a synergistic toughening for epoxies containing rubber particles in conjunction with solid glass spheres. The source of the synergism was found to be the stretching of the plastic zone as the result of interactions of the stress field near the crack tip and the solid glass particles when the two modifiers were physically close together. Rubber particles engulfed in these overlapping stress fields were subjected to stresses high enough to promote cavitation and shear yielding mechanisms.

Similar to a soft/hard hybrid system, synergistic toughening has been reported in epoxies containing a combination of two soft particles, such as rubber and hollow glass spheres[11] and coarse and fine rubber particles.[12,13] Azimi et al.[11] investigated K_{IC} of a hybrid epoxy composite containing rubber and hollow glass spheres. In their experiments, the volume fractions of the rubber and the glass sphere varied when a total volume fraction of modifiers of 10% was maintained. Synergistic toughening was observed for some rubber/glass sphere formulations. Chen and Jan[12] found that epoxies containing large

Correspondence to: R. Bagheri (rezabagh@sharif.edu).
Contract grant sponsor: Iranian Fuel Conservation Organization.

and small rubber particles exhibited a toughness that was greater than that of the additive rule. Bagheri et al.[13] reported synergistic toughening in an epoxy modified with bimodal size rubbers. These investigators claimed that plastic-zone branching was responsible for the observed synergism. According to this study, fine particles cavitated in the process zone ahead of the crack tip, and coarse rubber particles acted as stress concentrators that caused branching, that is, enlargement, of the plastic zone.[13]

On the basis of what has been reported, synergistic toughening in rubber-modified blends containing bimodal sized particles might be expected. However, questions remain regarding the influences of the matrix ductility, the strain rate, the cavitation resistance of the rubbery phase, the size ratio of the two modifiers, and so on. This particular investigation was designed to examine the concept of synergistic toughening in a system similar to that in a previous study[13] with a more brittle matrix. Therefore, two types of rubber modifiers, including amine-terminated butadiene acrylonitrile (ATBN) rubber and recycled rubber particles, were incorporated into a diglycidyl ether of bisphenol A (DGEBA) epoxy.

EXPERIMENTAL

Materials

The model system used in this study was based on DGEBA epoxy with an epoxy equivalent weight of 170 g/equiv (Araldite LY564) from Huntsman (Basel, Switzerland), and the curing agent used was cycloaliphatic polyamine hardener (HY22962) from Vantico (Basel, Switzerland). The modifying agent was ATBN copolymer (Hycar1300x16), with 16% acrylonitrile, an amine equivalent weight of 900, and a molecular weight of 3600, from Noveon Inc. (Cleveland, Ohio, USA). Recycled rubber particles were from common ground tire from Dena Co. (Shiraz, Iran), with an approximate nominal particle size of 150 μm. Throughout the article, recycled rubber is called *tire*, for simplicity.

Processing

A stoichiometric ratio of the curing agent and resin were mixed for 10 min; this was followed by degassing at room temperature for about 20 min. The solution was then cast into a 5 mm thick glass mold at room temperature. The cast material was cured for 6 h at 90°C in a circulating air oven. The same processing conditions were employed for all toughened epoxies as well. In single-modifier formulations, the modifier and epoxy were mixed at room temperature *in vacuo* for 30 min before the curing agent was added. In the case of hybrid systems, ATBN was mixed for 30 min with epoxy before tire particles were added. The blend was then mixed for 10 min before the addition of the curing agent. Table I presents the formulations.

TABLE I
Formulations Made in This Study

Designation	ATBN content (phr)	Tire content (phr)	HY22962 (g)	LY564 (g)
Neat	0	0	25	100
T10	0	10	25	100
A2.5/T7.5	2.5	7.5	25	100
A5/T5	5	5	25	100
A*10[a]	7.5	2.5	25	100
A10	10	0	25	100

[a] For simplicity, the formulation containing 7.5-phr ATBN and 2.5-phr tire is called A*10.

Characterization techniques

The glass-transition temperatures (T_g's) of the samples were determined with a differential scanning calorimeter with a TA Instruments (New Castle, Delaware, USA). The 7-mg samples were scanned in the range 60–130°C at a heating rate of 10°C/min. The specimens were contained in aluminum cans and tested in a helium atmosphere. Plane strain K_{IC} was determined with single-edge-notch (SEN) specimens tested in three-point-bending (3PB) geometry. Specimens with a thickness of 5 mm were used for this test. The ASTM D 5045 guideline was followed to measure K_{IC}. Precracks were introduced by hammering with a razor blade chilled in liquid nitrogen. The K_{IC} values reported represent averages of a minimum of five tests. The following relations were used to calculate K_{IC}:

$$K_{IC} = \frac{Ps}{tw^{3/2}} f(a/w) \tag{1}$$

$$f(X) = \frac{3X^{1/2}[1.99 - X(1-X)(2.15 - 3.93X + 2.7X^2)]}{2(1+2X)(1-X)^{3/2}} \tag{2}$$

where P is the maximum load at the instance of crack initiation, t is the thickness of the specimen, s is the span width, w is the width of the specimen, a is the initial crack length, and $f(X)$ is the nondimensional shape factor where X is the same as a/w ($X = a/w$). The tensile properties of the resin were determined according to ASTM D 638.

Fractography

Fracture surfaces of the SEN–3PB specimens were examined with scanning electron microscopy (SEM) at an accelerating voltage of 20 kV. The samples were coated with a thin layer of gold before

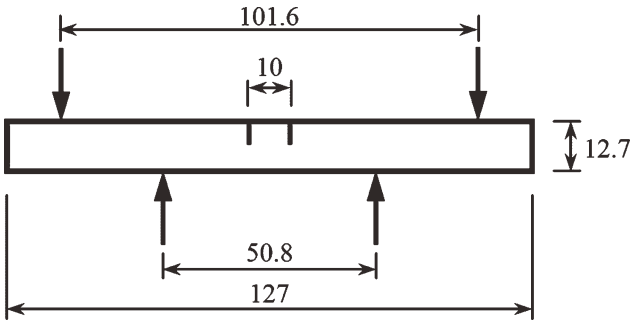

Figure 1 Schematic of the DN–4PB specimens used for observation of the crack-tip damage zone. All of the dimensions are in millimeters.

examination. To observe the crack-tip damage zone of the modified epoxies, a double-notched (DN)–four-point bending (4PB) method, in conjunction with transmission optical microscopy (TOM), was employed. Details of this technique are as follows: first, two edge cracks of equal length were introduced into a bending sample (Fig. 1). The specimen was loaded in a 4PB fixture at crosshead speed of 5 mm/min until a damage zones formed at the crack tips. Finally, one of the cracks that first reached the instability point propagated, and the sample fractured. The other crack that was unloaded and, therefore, contained a well-developed damage zone represented the conditions before the failure of the material. This damage zone could be observed with a TOM after thinning via petrographic polishing. Thin specimens ($\sim$ 150 μm) taken from the midplanes of the 4PB samples were used.

RESULTS AND DISCUSSION

K_{IC} test

The results of K_{IC} measurements are listed in Table II. These results are further illustrated in Figure 2, where K_{IC} is shown versus the modifier composition.

Although the incorporation of 10-phr tire alone enhanced K_{IC} only by 20%, the addition of 10-phr ATBN improved K_{IC} of the resin by 230%. As shown in Figure 2, A2.5/T7.5 and A5/T5 almost followed the rule of mixtures. However, Table II shows a significant increase (250%) in the K_{IC} value for A*10; this was a positive deviation from the rule of mixtures. Interestingly, the K_{IC} value of this material was higher than that of A10. Therefore, synergistic toughening occurred when 7.5-phr ATBN and 2.5-phr tire were incorporated. This result was similar to the findings of previous researchers, who reported a positive deviation from the rule of mixtures in rubber-toughened polymers when bimodal sized rubber particles were incorporated.[12,13] This difference in K_{IC} values was attributed to the interaction of the large particles (tire particles) with small ones (ATBN) in the vicinity of the crack tip.[12,13]

TABLE II
K_{IC} Values of the Two-Phase Resin

Sample	K_{IC} (MPa·m$^{0.5}$)
Neat	0.5 ± 0.03
T10	0.6 ± 0.05
A2.5/T7.5	0.75 ± 0.07
A5/T5	1 ± 0.04
A*10	1.75 ± 0.07
A10	1.65 ± 0.11

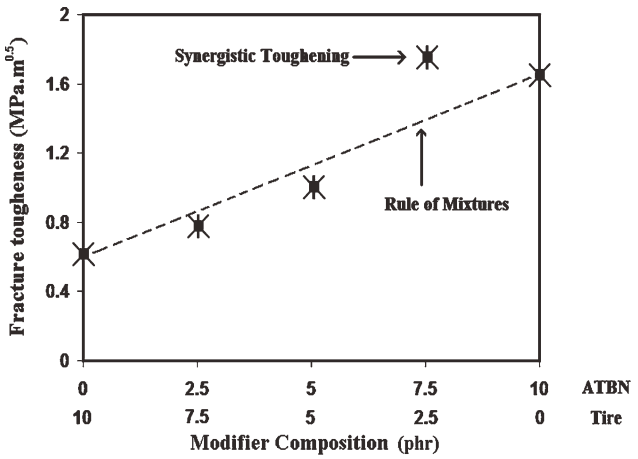

Figure 2 K_{IC} versus the blend composition. Synergistic toughening was evident in 7.5-phr ATBN/2.5-phr tire (A*10).

T_g evaluation

To further study the behavior of hybrid epoxies, the variations of the T_g values of the neat, A10, and A*10 specimens were measured. The results are shown in Table III. As shown, the introduction of modifiers led to a slight decrease in T_g. Table III also shows that T_g of A*10 was slightly higher than that of A10. The reduction in T_g of the epoxy with the addition of liquid rubber could be attributed to the lack of complete precipitation of the rubber molecules from the epoxy resin.[4] Please note that dissolved rubber molecules could plasticize the epoxy resin and, thus, reduce its T_g.[4] These findings reveal that the source of the high K_{IC} of A*10 (Table II) was not the rubbers' high ability to plasticize the resin.

TABLE III
T_g Values of the Resins

Sample	T_g (°C)
Neat	109
A10	106.1
A*10	107.3

Tensile testing

The tensile properties of the neat, A10, and A*10 specimens were examined, and their stress–strain graphs were obtained. The results are shown in Figure 3. As shown in this figure, both rubber-modified epoxies had lower elastic moduli than the neat resin. This could be explained by the low Young's moduli of the rubbery materials. Figure 3 also shows brittle behavior in the neat and A*10 specimens with very limited elongation before fracture, whereas in the case of the A10 specimen, a rather ductile manner was observed. The high ductility of the A10 specimen could be explained by means of a stress concentration effect of ATBN particles, which enhanced shear yielding in the epoxy matrix.

Comparing the K_{IC} and tensile test results, one may see a discrepancy where A*10 behaved in a very tough manner in K_{IC} testing (Table II), whereas the same material was extremely brittle in the tensile tests (Fig. 3). This means that the source of the high K_{IC} of A*10 (Table II) was not the high capability of plastic deformation.

To determine an appropriate explanation for the high K_{IC} of A*10, microscopic techniques were used. This task is discussed in the following sections.

SEM

Figure 4 presents the SEM micrographs taken from the fracture surface of the SEN–3PB specimens. The unmodified specimen had the smoothest fracture surface [Fig. 4(a)] because of the lack of plastic deformation. Similarly, the fracture surface of T10 showed limited surface roughness; this indicated a lack of severe plastic deformation in this material [Fig. 4(b)]. This observation was parallel to the K_{IC} data shown in Table II, where the neat and T10 specimens had very close K_{IC} values. In the case of the A10 specimen, which is shown in Figure 4(c), a large amount of roughness was observed, which could be attributed to the significant plastic deformation at the crack tip.

Figure 4(d) illustrates the fracture surface of the A*10 specimen. A comparison of Figures 4(c) and 4(d) revealed less roughness on the fracture surface of A*10 compared to A10; this indicated less plastic deformation in A*10, whereas Table II presents a higher K_{IC} of A*10 compared to A10. This means that the toughening mechanisms in A*10 and A10 might have been different. Figure 4(d) reveals poor interfacial adhesion between the tire particles and the matrix. However, earlier investigations showed that the rubber–matrix adhesion was not a dominant factor in the K_{IC} of rubber modified epoxies because of the small elastic modulus of rubber particles.[4] Looking at Figure 4(d), we observed stepwise surfaces in the vicinity of the tire particles as the result of interaction between the crack tip and tire particles.

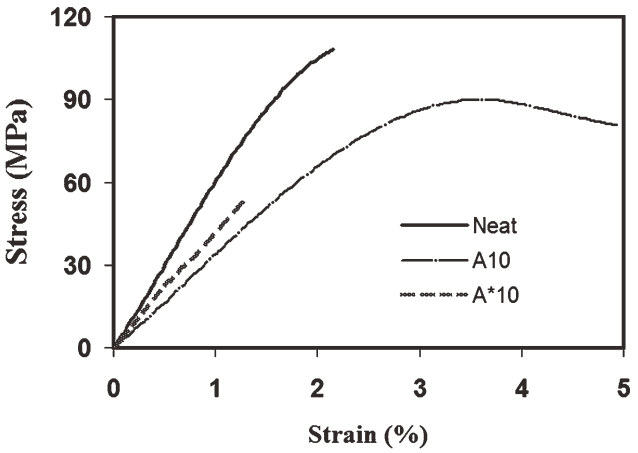

Figure 3 Stress–strain curves for the neat, A10, and A*10 samples.

To further analyze the difference in the fracture behavior of the A10 and A*10 specimens, higher magnification images were taken via SEM, and they are shown in Figure 5. Figure 5(a) contains the same micrograph shown in Figure 4(c) taken at a higher magnification. This figure represents a uniform dispersion of cavitated ATBN particles with 1-μm mean diameters.

Cavitation and concomitant shear yielding are one of the major mechanisms of energy absorption in toughened epoxies.[6–7] The amounts of cavitation and void growth can be determined from the volume fractions of nonmatrix portions of the fractured surfaces; these were calculated from the SEM micrographs (Fig. 5) with image-analysis techniques. Figure 5(a) shows that the volume fraction of the nonmatrix portion was approximately 19% through most of the whitening zone of A10. It was higher than the volume fraction of the ATBN particles (10.5%) calculated from the composition and densities of the modified resin components. Therefore, the extent of cavitation for this material was about 80%.

Figure 5(b) shows the higher magnification of Figure 4(d), which represents fracture surface of the A*10 specimen. As shown, ATBN particles were cavitated near the tire particles. The volume fraction of nonmatrix portions of A*10 was approximately 12% near tire particles at the crack tip. Note that the volume fraction of the ATBN portions was approximately 8%, as calculated from the composition and densities of the hybrid resin components. The extent of cavitation in A*10 was thus 50%.

A comparison of the extent of cavitation calculated from Figure 5(a,b), similar to what is shown in Figure 4, revealed a possible difference in the toughening mechanisms of the A10 and A*10 specimens. Please note that lower cavitation of A*10 was in

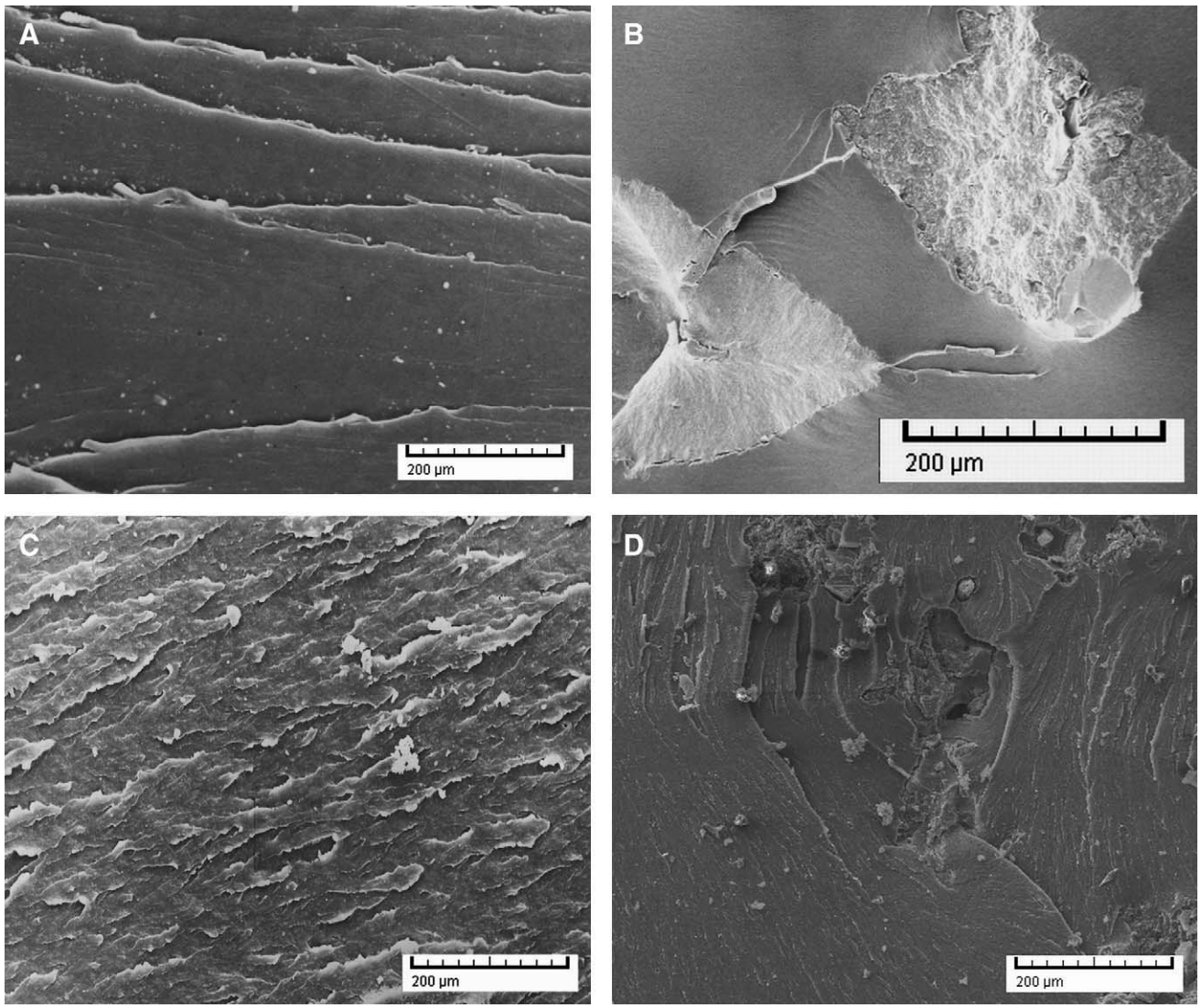

Figure 4 SEM photos taken from the damaged surfaces of the samples: (a) neat, (b) T10, (c) A10, and (d) A*10.

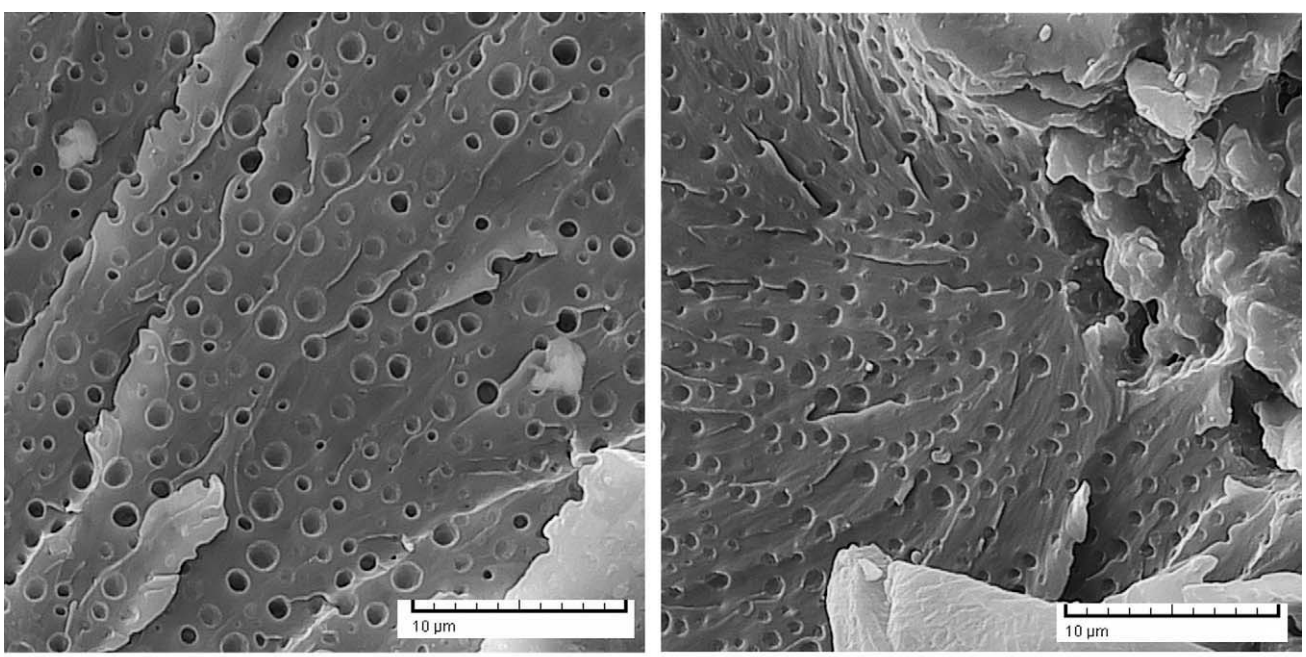

Figure 5 SEM photos taken from the damaged surface of the samples: (a) A10 and (b) A*10.

contradiction with the exception of higher plastic deformation as the source of synergism observed. However, SEM is not a definitive technique for judgment of the toughening mechanism. Therefore, TOM was used to investigate the subsurface damage and explore the exact toughening mechanism(s), as discussed in the following section.

TOM

Figure 6 shows TOM micrographs taken from the crack-tip damage zones of DN–4PB of the T10, A10, and A*10 specimens. This figure shows a major difference in toughening mechanisms in the three materials. Figure 6(a) shows no evidence of a process zone at the crack tip of T10. The crack-tip damage zone of A10 shown in Figure 6(b) is typical for rubber-toughened epoxies, where the cavitated particles induce massive shear deformation. The TOM micrograph shown in Figure 6(c) illustrates massive crack deflection and branching at the crack tip of A*10.

As shown, the shape and size of the damage zones were significantly different in the A10 and A*10 specimens. Although an elliptical shape damage zone, that is, typical of plastic deformation, is shown in Figure 6(b), Figure 6(c) illustrates a highly branched damage zone, where the crack deflects and branches toward the large rubber particles. This observation was consistent with the differences observed in the SEM micrographs (Figs. 4 and 5).

Higher magnification TOM images than those shown in Figure 6 are shown in Figure 7. This figure illustrates similar features to those shown in Figure 6. In the case of T10, however, a weak sign of crack bridging was seen in the crack wake [arrow in Fig. 7(a)]. Because crack bridging is not considered a major toughening mechanism in rubber-modified epoxies,[4] this observation may not be taken as a serious toughening mechanism. The K_{IC} data reported in Table II supported this claim, where the T10 and neat specimens showed almost identical K_{IC} values.

The elliptical damage zone shown in Figure 7(b) was similar to that reported by previous investigators;[14] this indicated massive shear yielding at the crack tip. The massive shear yielding occurring in this material accounted for the higher K_{IC} of A10 versus T10. Figure 7(c) illustrates the crack-branching phenomenon at the crack tip, which was observed at lower magnification [Fig. 6(c)] as well. This figure, however, shows the formation of a small elliptical damage zone at the tip of one of the crack branches [arrow in Fig. 7(c)].

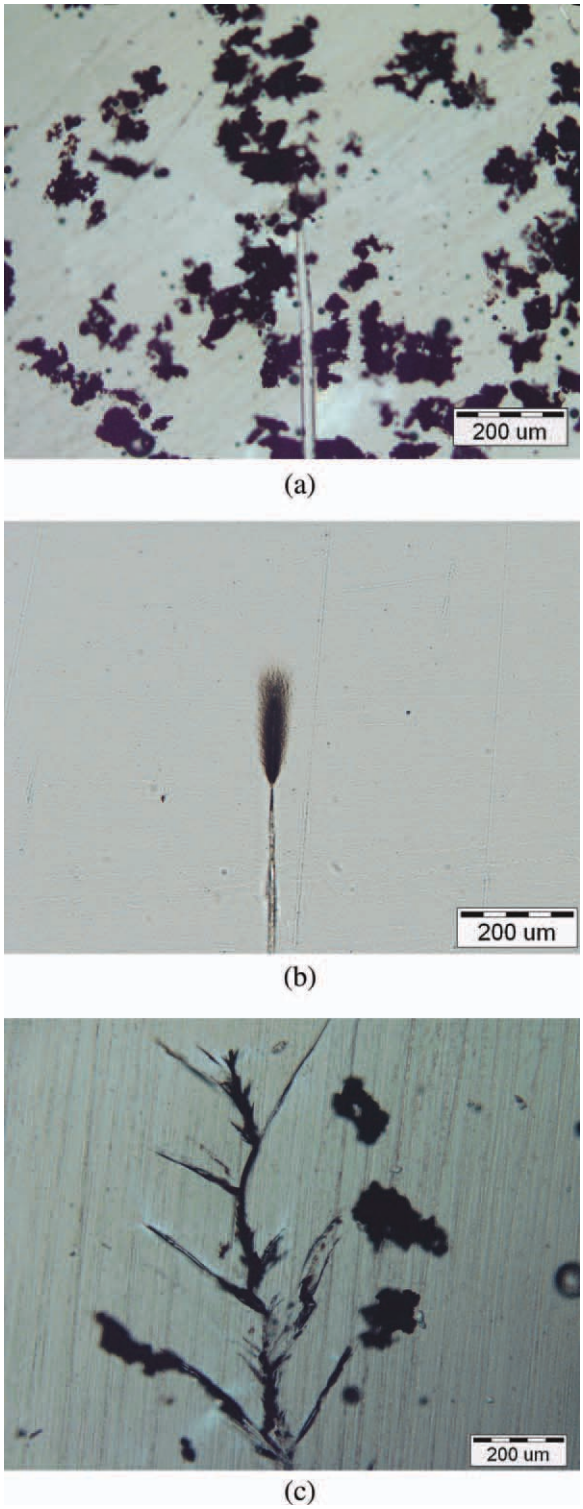

Figure 6 TOM micrographs taken from the midplane of the crack-tip damage zones of (a) T10, (b) A10, and (c) A*10 under bright-field conditions. The crack-growth direction was from bottom to top. [Color figure can be viewed in the online issue, which is available at wileyonlinelibrary.com.]

Toughening mechanisms

TOM micrographs (Figs. 6 and 7) revealed that the major toughening mechanism in A*10 was crack branching. Crack branching redistributes stresses at the branch tips and increases the energy needed to propagate a crack through the material, thereby

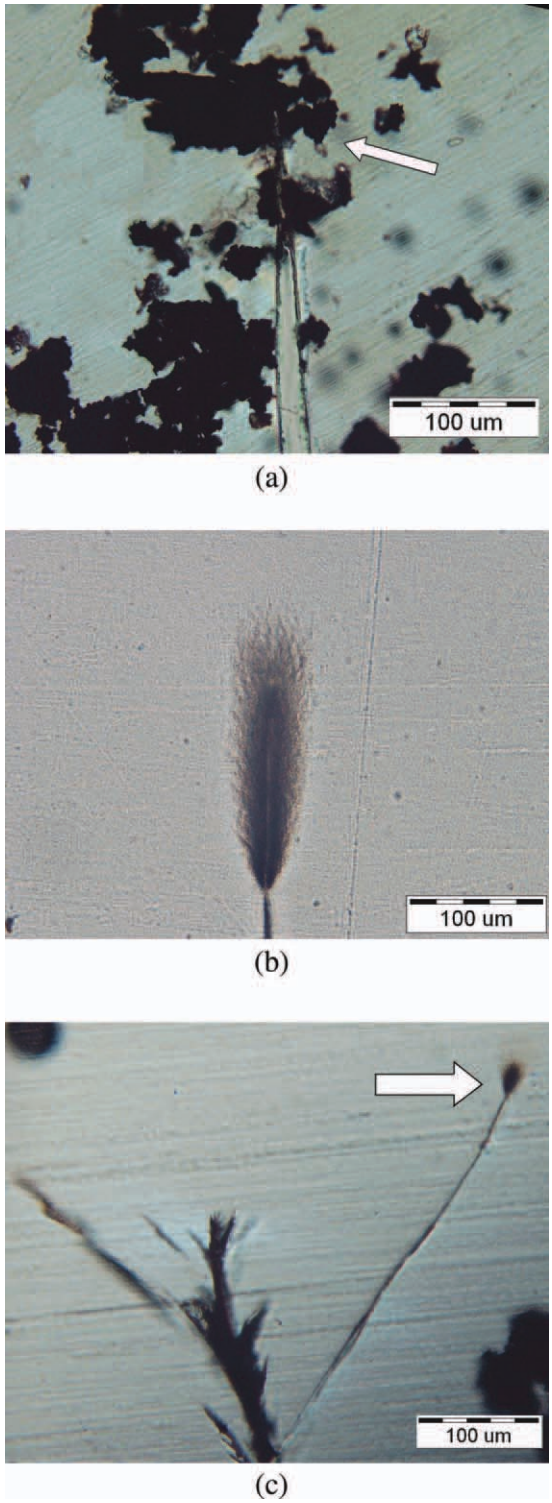

Figure 7 TOM micrographs taken from the crack wakes of the (a) T10, (b) A10, and (c) A*10 specimens at higher magnifications. [Color figure can be viewed in the online issue, which is available at wileyonlinelibrary.com.]

resulting in improved K_{IC} values. The best known parameter to describe the contribution of crack branching and the resulting mode mixity to the overall toughness of material is the strain energy release rate (G). Assuming the crack branches, one can no longer describe the crack-tip stress field by the nominal mode I stress intensity factor because the mode mixity occurs at the crack branch tip, and thus, G decreases dramatically.[15–17] This, in turn, implies that the crack-growth resistance of a material having crack-branching characteristic is higher than that of the same material without such a characteristic. This approach is commonly used to explain toughening mechanisms, such as branching and crack deflection, in modified epoxies.[15–17] However, more experimental data is required to develop an accurate quantitative model.

We might have also considered the increase in the fracture surface to be due to the crack branching responsible for improved K_{IC} in A*10. However, this claim might be argued by the very modest contribution of surface energy to the K_{IC} of engineering materials.[18] Another hypothesis to explain the improved toughness with crack branching may be proposed by consideration of the generation of several damage zones at the branch tips. Please note that formation of several damage zones at the branch tips, as shown in Figure 7(c), may have a positive effect on the total energy absorption before fast fracture.

It would be interesting to explore the reason why crack branching occurred in the A*10 specimen. The crack branching shown in Figures 6(c) and 7(c) could be explained via the following rationale. The tire particles acted as large stress concentrators in the vicinity of the crack tip. The highly stressed ligaments between the crack tip and the tire particles fractured when they no longer supported the induced tensile stresses.[19] Crack branches then formed and propagated toward the tire particles, and thus, the crack-branching zone formed at the main crack tip.

The question remains as to why this scenario did not occur in the T10 specimen. The answer lies in the role of fine ATBN particles distributed within the ligament between the large tire particles and the crack tip in the hybrid system. We hypothesized that the ATBN particles restricted unstable crack propagation within the ligament, and thus, the branched crack sustained even higher stresses than that the unmodified epoxy matrix could tolerate. Therefore, a much higher K_{IC} could be expected in A*10 compared to T10, where no ATBN particle existed within the aforementioned ligaments.

Comparison with a similar system

As mentioned earlier, Bagheri et al.[13] reported synergistic toughening in a similar system. They used recycled rubber particles (R4200) with a nominal particle size of 75 μm in cooperation with a carboxyl-terminated butadiene acrylonitrile (CTBN)

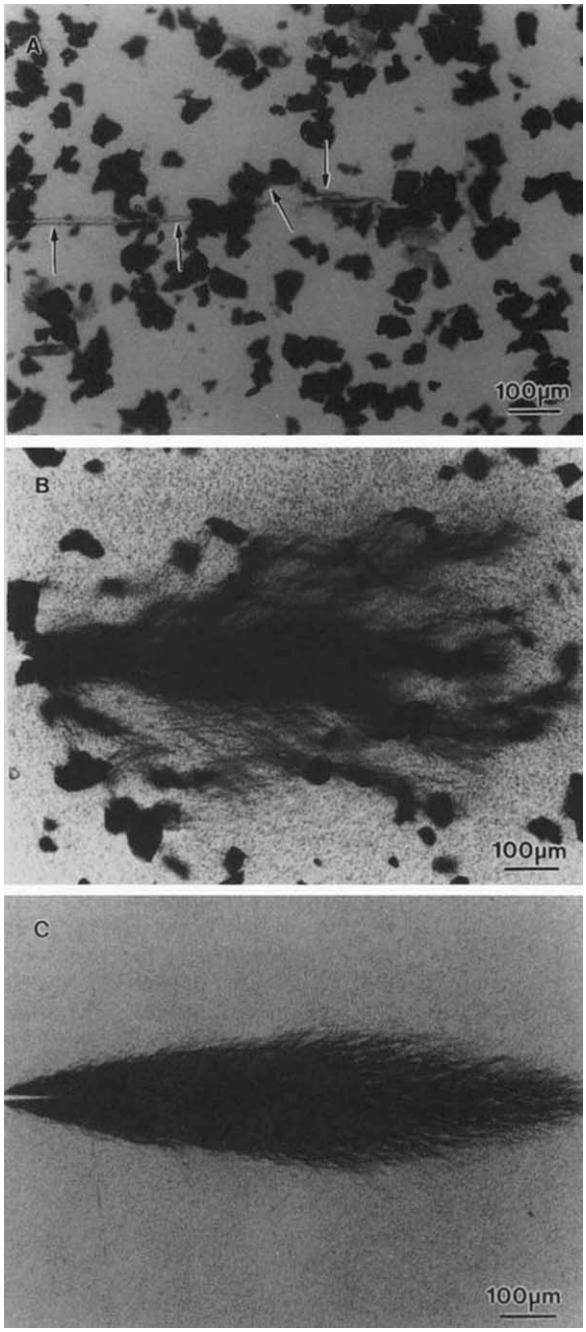

Figure 8 TOM micrographs taken from the crack wakes of the (a) recycled-rubber-modified, (b) hybrid-modified, and (c) CTBN-modified systems.[13]

reactive liquid rubber for the toughening of the epoxy. Bagheri et al.[13] used a DGEBA epoxy with a Piperidine hardener (DGEBA/PIP). Their results reveal synergistic toughening when 2.5-phr recycled rubber and 7.5-phr CTBN were incorporated. Although large recycled rubber particles were less effective than small CTBN particles in the toughening of the epoxy matrix, the blending of the two modifiers resulted in synergistic toughening.

Figure 8 illustrates the TOM micrographs taken from the crack tips. Figure 8(a) reveals that when used alone, recycled rubber particles simply acted as large stress concentrations and modestly contributed to toughening via crack deflection and microcracking. The crack path is shown by arrows in Figure 8(a). Micrometer-sized CTBN particles produced higher toughness via cavitation and concomitant massive shear yielding in the matrix [Fig. 8(c)]. However, in the presence of CTBN, the recycled particles acted as stress concentrators and stretched shear bands to distances far from the crack tip [Fig. 8(b)]. This mechanism caused plastic-zone branching and provided an unexpectedly high K_{IC} value.

The concept of synergism in hybrid epoxy systems was raised in both this study and in the earlier work by Bagheri et al.[13] Despite the similarities between the two investigations, a major difference was seen in the toughening mechanisms observed. As shown in Figures 6(c) and 8(b), synergistic toughening is associated with enlargement of the damage zone due to the interaction of the large rubber particles with the crack tip. However, the natures of the mechanism were different in the two studies. Although the earlier work showed plastic-zone branching at the crack tip, in this study, the enlargement of the damage zone occurred via crack branching.

To interpret this different behavior, one may consider the difference in ductility of the two epoxy systems used in two investigations. Comparing the K_{IC} data obtained in two studies, one can conclude that the epoxy system used in the earlier study[13] was more toughenable than the system used in this study (See Table IV). This was why the damage zone size was much larger in Figure 8(c) than that shown in Figure 6(b). When the large rubber particles were incorporated into the hybrid system, the stress field at the crack-tip changed, and on the basis of the results of both studies, the stress was concentrated in the ligaments between the crack tip and the large particles. In the more ductile epoxy system, then, the ligaments underwent shear deformation. Therefore, plastic-zone branching occurred [Fig. 8(c)]. In the less ductile matrix, however, the ligaments could not accommodate shear deformation and fracture. As a result, crack branching occurred at the crack tip [Fig. 7(c)].

The interesting point, found in a comparison of the results of this study with those of an earlier work,[13] was that damage-zone enlargement via branching could have been the source of synergistic toughening in the hybrid epoxy blends. It seemed

TABLE IV
Comparison Between the K_{IC} Values of the Two Systems

Sample	K_{IC} (MPa·m$^{0.5}$)
Neat	0.5
DGEBA/PIP[a]	0.98

[a] Ref. 13.

not to matter whether the enlargement occurred via plastic-zone branching or crack branching. Further elucidation of synergistic toughening in hybrid epoxy blends will be the subject of ongoing research in this group and will be presented in part II of this article series.

CONCLUSIONS

A DGEBA epoxy was toughened by two different sizes of rubber modifiers to produce synergistic toughening with a commonly used reactive liquid elastomer, ATBN, and recycled tire particles. Although the total rubber content in the toughened blends was kept constant at 10 phr, the ratio between the two modifiers was varied. The results of K_{IC} testing of the blends revealed synergistic toughening when 2.5-phr tire and 7.5-phr ATBN were incorporated. TOM fractography of the hybrid system showed crack branching to be responsible for the synergism observed. It seemed that the crack branching occurred as a result of interaction between the crack-tip stress field and those of the large particles. The crack branches stretched from the crack tip toward the large particles and resulted in an enlargement of the damage zone and thus, enhanced the crack-growth resistance. It should be also noted that when the crack branched, the crack-tip stress field could no longer be described by the nominal mode I stress intensity factor due to the mode mixity at the crack tip, and the total G decreased significantly. Comparing the results of this study with those of earlier investigations, one may appreciate the important role of matrix ductility on the nature of the crack-tip damage zone in hybrid epoxies. Although synergism occurs by crack branching in brittle matrices, hybrid blends having a ductile matrix may show synergistic toughening due to plastic-zone branching.

The authors are thankful to Pooyan Motamedi, Saeed Zokaei, and Rasool Lesankhosh for their laboratory associations.

References

1. Kinloach, A. J.; Shaw, S. J.; Tod, D. A.; Huntston, D. L. Polymer 1983, 24, 1341.
2. Pearson, R. A.; Yee, A. F. J Mater Sci 1991, 26, 3828.
3. Sue, H. J.; Garcia-Meitin, E. I.; Pickelman, D. M. In Polymer Toughening; Arends, C. B., Ed.; Marcel Dekker: New York, 1996; Chapter 5.
4. Bagheri, R. Ph.D. Dissertation, Lehigh University, 1995.
5. Bagheri, R.; Pearson, R. A. J Mater Sci 1996, 31, 3945.
6. Bagheri, R.; Pearson, R. A. Polymer 1996, 37, 4529.
7. Bagheri, R.; Pearson, R. A. Polymer 2000, 41, 269.
8. DiBeradino, M. F.; Pearson, R. A. In Toughening of Plastics—Advances in Modeling and Experiments; ACS Symposium Series 759; Pearson, R. A., Sue, H. J., Yee, A. F., Eds.; American Chemical Society: Washington, DC, 2000; Chapter 13.
9. Kinloch, A. J.; Maxwell, D. L.; Young, R. J. J Mater Sci 1985, 20, 4169.
10. Azimi, H. R.; Pearson, R. A.; Hertzberg, R. W. J Appl Polym Sci 1995, 58, 449.
11. Azimi, H. R.; Pearson, R. A.; Hertzberg, R. W. Polym Eng Sci 1996, 36, 2352.
12. Chen, T. K.; Jan, Y. H. J Mater Sci 1992, 27, 111.
13. Bagheri, R.; Williams, M. A.; Pearson, R. A. Polym Eng Sci 1997, 37, 245.
14. Arias, M. L.; Frontini, P. M.; Williams, R. J. J. Polymer 2003, 44, 1537.
15. Faber, K. T.; Evans, A. G. Acta Metall 1983, 31, 565.
16. Yan, X. J Appl Mech 2005, 72, 330.
17. Kitagawa, H.; Yuuki, R.; Ohira, T. Eng Fracture Mech 1975, 7, 515.
18. Hertzberg, R. W. Deformation and Fracture Mechanics of Engineering Materials; Wiley: New York, 1996.
19. Lazzeri, A.; Bucknall, C. B. In Toughening of Plastics—Advances in Modeling and Experiments; ACS Symposium Series 759; Pearson, R. A., Sue, H. J., Yee, A. F., Eds.; Oxford University Press: New York, 2000; Chapter 2.